BIOCHEMISTRY
including biophysical chemistry & molecular biology

Rapid Report

pubs.acs.org/biochemistry

Pathogenic C9ORF72 Antisense Repeat RNA Forms a Double Helix with Tandem C:C Mismatches

David W. Dodd,[†] Diana R. Tomchick,[‡] David R. Corey,[†,§] and Keith T. Gagnon*[,∥,⊥]

[†]Department of Pharmacology, [‡]Department of Biophysics, and [§]Department of Biochemistry, University of Texas Southwestern Medical Center, Dallas, Texas 75390, United States

[∥]Department of Biochemistry and Molecular Biology, School of Medicine, and [⊥]Department of Chemistry and Biochemistry, Southern Illinois University, Carbondale, Illinois 62901, United States

Supporting Information

ABSTRACT: Expansion of a GGGGCC/CCCCGG repeat sequence in the first intron of the *C9ORF72* gene is a leading cause of frontotemporal dementia (FTD) and amyotrophic lateral sclerosis (ALS). In this combined disorder, called c9FTD/ALS, the expansion is bidirectionally transcribed into sense and antisense repeat RNA associated with disease. To better understand the role of C9ORF72 repeat RNA in molecular disease pathology, we determined crystal structures of a [$(CCCCGG)_3(CCCC)$] model antisense repeat RNA to 1.47 Å resolution. The RNA structure was an A-form-like double helix composed of repeating and regularly spaced tandem C:C mismatch pairs that perturbed helical geometry and surface charge. Solution studies revealed a preference for A-form-like helical conformations as the repeat number increased. Results provide a structural starting point for rationalizing the contribution of repeat RNA to c9FTD/ALS molecular disease mechanisms and for developing molecules to target C9ORF72 repeat RNA as potential therapeutics.

At least 25 neurological disorders are caused by expansion of microsatellite repeats in the human genome.[1,2] For most of these disorders, an RNA is transcribed across the repeat expansion to produce coding or noncoding transcripts. These expanded repeat RNAs can become trapped as focal aggregates inside cell nuclei or be translated into repetitive polypeptides in the cytoplasm. The consequences of these two pathways are believed to drive disease pathology by various mechanisms, including depletion of RNA binding proteins by sequestration[3,4] and mimicking protein motifs that compete with normal protein function.[5] Because expression of expanded repeat RNA is the root cause of severe diseases that currently lack good treatment options, understanding the fundamental role of RNA structure in aggregation, protein binding, localization, and translation is important for understanding pathology and drug discovery.

Previous crystal structures of repeat expansion RNA have primarily focused on minimal CNG trinucleotide repeat RNAs, where N represents either A, U, C, or G bases. Repeat RNA structures have revealed a common theme of A-form-like duplexes, typically with a pattern of single N:N bulges spaced between two Watson−Crick base pairs.[6] Recent structures of more complex CCUG repeat RNA[7,8] implicated in myotonic dystrophy type 2 and AUUCU repeat RNA[9] implicated in spinocerebellar ataxia type 10 have revealed tandem C:U/U:C mismatches between G-C base pairs and three mismatches between A-U base pairs, respectively. Structural characterization of CUG repeat RNA has successfully led to design of small molecules that can block sequestration of MBNL-1 protein, a key disease mechanism in myotonic dystrophy type 1.[10]

It was recently found that expansion of a GGGGCC/CCCCGG hexanucleotide repeat in the first intron of the *C9ORF72* gene is the leading genetic cause of two neurological disorders, frontotemporal dementia (FTD) and amyotrophic lateral sclerosis (ALS). In this combined disease, commonly known as c9FTD/ALS, the expanded repeat is transcribed bidirectionally, generating noncoding sense $(GGGGCC)_n$ RNA or antisense $(CCCCGG)_n$ RNA.[11] Foci composed of sense and antisense expRNA are both detected in c9FTD/ALS cell nuclei.[11,1213] In addition, repeat-associated non-AUG (RAN) translation produces poly-dipeptides from both repeat RNAs in c9FTD/ALS.[13−15] The repeat RNAs have also been implicated in disease-associated R-loop formation at the *C9ORF72* locus.[16] These phenomena are currently implicated in the molecular pathology of c9FTD/ALS, and molecules that selectively interfere with RNA structure or protein interactions would be lead compounds for drug development.

Although the $(GGGGCC)_n$ sense RNA has been predicted to possess G-quadruplex structure,[17,18] the structure for the $(CCCCGG)_n$ antisense RNA has not been investigated. C-Rich sequences can often assume i-motif (tetraplex) or triplex structures at low pH but are not expected to be stable at physiological pH.[19] Alternatively, formation of a duplex would have to accommodate excess non-Watson−Crick paired cytosine. Thus, how the C9ORF72 antisense RNA folds and the potential impact of its structure on disease pathology and small molecule targeting has remained unclear.

To better understand the role of antisense repeat RNA structure in c9FTD/ALS and provide a starting point for RNA-targeted therapeutics, we determined two very similar crystal structures of a [$(CCCCGG)_3(CCCC)$] C9ORF72 antisense repeat RNA. Our model RNA was composed of approximately four repeats, lacking only the final two G nucleotides of the fourth repeat (Figure 1A). We reasoned that this minimal sequence would be sufficient to form a variety of possible duplex, triplex, or tetraplex RNA structures.

Received: February 15, 2016
Published: February 15, 2016

DOI: 10.1021/acs.biochem.6b00136
Biochemistry 2016, 55, 1283−1286

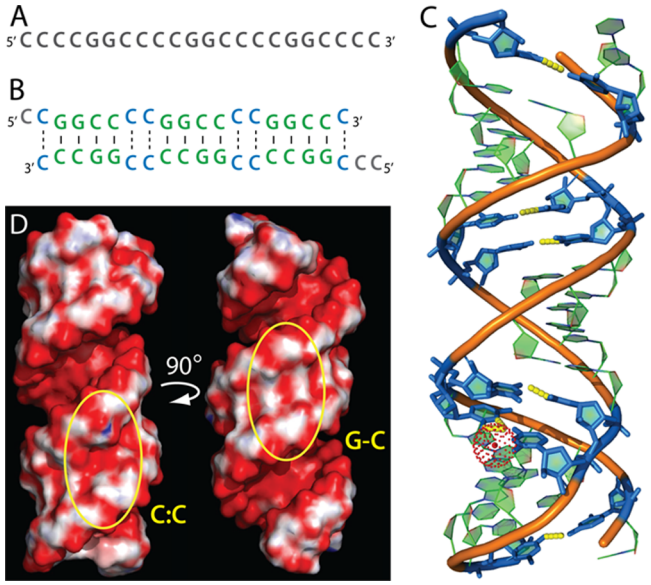

Figure 1. C9ORF72 antisense repeat RNA fragments form an A-form-like double helix with tandem C:C mismatches and perturbed surface charge. (A) Model C9ORF72 antisense repeat RNA sequence used for crystal screening. (B) Secondary structure representation of determined crystal structures. Canonical Watson−Crick pairs are colored green with solid lines, and C:C pairs are colored blue with dotted lines. (C) Global architecture of the crystal A structure. Watson−Crick G-C pairs are colored green, and tandem C:C mismatch pairs are colored blue. Hydrogen bonds are colored yellow. A coordinated strontium ion is shown with red dots. (D) Changes in electrostatic surface charge at C:C pairs compared to canonical G-C base pairs.

Screening under varied conditions of pH, ionic strength, and RNA concentration resulted in two isomorphous crystals that diffracted to 1.47 Å (crystal A) and 1.75 Å (crystal B). The repeat RNA adopts a double-stranded A-form-like helical structure characterized by repeating units of four Watson−Crick G-C/C-G base pairs separated by two tandem C:C pairs (Figure 1B,C). These structures are among the longest contiguous atomic-resolution X-ray structures of repeat expansion RNA and appear to be the only hexanucleotide repeat RNA crystal structures reported to date and the only RNA structure containing tandem C:C mismatches within a Watson−Crick-paired helix.[6,20] Primary lattice contacts for both crystals were perpendicular to the helical axis, which prevented helical stacking of duplexes. Lack of electron density for terminal cytosine residues, capable of forming additional C:C pairs, indicated conformational disorder and low stability at helix termini. Although slipped structures are possible, base pairing of the double helix maximized the number of Watson−Crick G-C pairs while minimizing C:C pairing.[21] Superpositioning of crystal A and crystal B grown under similar conditions but in the presence of Sr^{2+} and Ba^{2+}, respectively, revealed nearly identical structures as evidenced by a root-mean-square deviation (rmsd) of 0.28 Å (Figure S1A). Both Sr^{2+} and Ba^{2+} coordinated to the same lattice contact within each crystal, indicating a strict requirement of these divalent cations for formation of the crystalline lattice (Figure S1B). Agreement between the two isomorphous structures supports the conclusion that the determined structure represents a stable conformer.

The presence of regularly spaced tandem C:C pairs perturbs the A-form architecture of the repeat RNA helix. Noncanonical C:C pairs altered the electrostatic surface potential when compared with normal Watson−Crick G-C/C-G base pairs (Figure 1D). Alterations were at the surface of the minor groove, which may impact putative interactions with RNA binding proteins. Similar changes in minor groove surface charge were previously observed in CCG RNA structures at single C:C mismatch pairs.[21]

The global helical architecture of our structure was classified as A-form by 3DNA analyses (ribose rings were in the expected C3′-*endo* sugar pucker conformation).[22] However, our structure deviated from a typical A-form helix in several respects (Table S1). Minor groove widths were smaller, while broader ranges for the major groove and overall helix width were observed. Base pair and base pair step parameters that were affected globally were the *propeller* and *opening*, whereas all other parameters, except base pair *slide* and *rise*, were affected locally at or nearby C:C pairs. Helical perturbations have been previously reported for other structures containing C:C pairs.[21,23] In our structure, some helical parameter changes can be explained by an apparent contraction of the helix width at tandem C:C pairs to accommodate hydrogen bonding distances between pyrimidine bases. This conclusion is supported by shorter average C1′−C1′ distances, with the smallest distances occurring at C:C pairs.

The high resolution of our structures allowed us to accurately model the cytosine bases of six C:C pairs in the electron density map (Figure 2A). Superimposing and overlaying all six C:C pairs

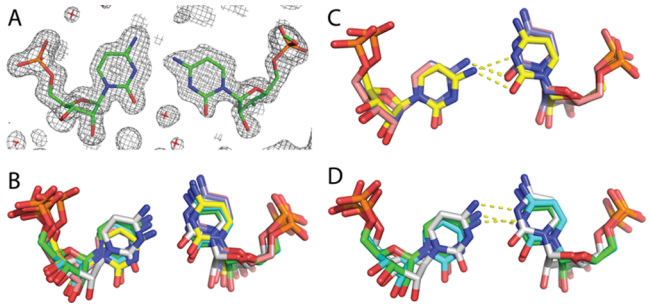

Figure 2. C:C mismatch pairs exhibit similar conformations and base interactions in C9ORF72 antisense repeat RNA. (A) Shown in gray mesh is the $|2mF_o - DF_c|$ electron density contoured at the 1.0σ level and superimposed on the stick representation of the refined coordinates of C16 (chain A, left) and C9 (chain B, right) of crystal A. (B) All six C:C pairs from crystal A are shown superimposed and overlaid. (C and D) Superpositioned and overlaid C:C pairs that form one of two major hydrogen bonding interactions in crystal A.

revealed consistent and reproducible formation of similar conformations and hydrogen bonding orientations (Figure 2B). The cytosine bases of each C:C pair established one of two hydrogen bond donor−acceptor interactions: a proton of the exocyclic amine interacting with either the opposing cytosine base's oxygen at position 2 (Figure 2C) or the lone pair of the nitrogen at position 3 (Figure 2D). One conformation observed for a C:C pair permits the possible formation of both hydrogen bonding configurations, which probably interconvert in solution (Figure 2C). Previous structures have been determined for RNAs containing single C:C mismatches, including a CCG repeat RNA, ribosome structures, and a hairpin from the human thymidylate synthase mRNA.[21,23] C:C pair conformation and hydrogen bonding in these studies conform overall to those observed in our structures. The unique nature of the CCCCGG hexanucleotide sequence, which allows four consecutive G-C/C-G base pairs to flank tandem C:C pairs, and the length of the

DOI: 10.1021/acs.biochem.6b00136
Biochemistry 2016, 55, 1283−1286

RNA helix likely contributes to the consistency and regularity of C:C pairing in our crystal structures.

To complement our atomic-resolution structural analysis, we tested the dependence of RNA structure on duplex length using circular dichroism (CD) spectropolarimetry and differential scanning calorimetry (DSC). CD reflects nucleic acid structure by detecting the absorbance of circularly polarized light expressed as units of molar ellipticity (millidegrees).[24] DSC can detect structural species and provide thermodynamic parameters and melting temperatures by measuring heat capacity changes as the temperature is increased.[25]

CD of $(CCCCGG)_n$ RNAs containing increasing numbers of repeats revealed shifts in spectra (Figure 3A). RNA composed of approximately two repeats, $[(CCCCGG)_1(CCCC)]$, exhibited a broad molar ellipticity peak centered around 275 nm with a shoulder around 290 and 250 nm. As the repeat number increased to nearly 10 repeats, $[(CCCCGG)_9(CCCC)]$, the peak at 275 nm shifted closer to 270 nm and became more prominent while the magnitude of the shoulder at 290 nm was reduced and the shoulder at 250 nm shifted to 240 nm and became more prominent. Annealing our four-repeat model RNA to a perfect complement $[(GGGGCC)_3GGGG]$ RNA to produce a perfect A-form duplex revealed a CD spectral peak near 265 nm with no substantial shoulders (Figure S2A). The small red-shift in absorbance (from the typical value of 260 nm) may be explained by the high cytosine content of our RNA.[26] Interestingly, CD of a $(CUG)_6$ repeat RNA, which is known to fold into an A-form-like helix with regular U:U mismatches,[27] had a molar ellipticity peak at 270 nm similar to the peak seen for $(CCCCGG)_n$ RNAs of higher repeat numbers (Figure S2A). Combined, these results indicate that alternative structures, possibly including slipped intermolecular and intramolecular states or noncanonical structures, may exist for $(CCCCGG)_n$ repeat RNAs. However, as the repeat number increases, a predominant A-form-like structure predominates.

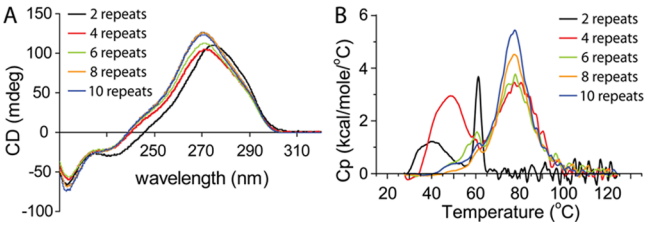

Figure 3. $(CCCCGG)_n$ RNA transitions to an A-form-like structure with increasing repeat numbers. Circular dichroism (A) or differential scanning calorimetry (B) for $(CCCCGG)_n$ RNAs of increasing size.

DSC analysis of $(CCCCGG)_n$ RNA composed of two repeats revealed at least two conformations with melting temperature (T_m) values of ~40 and 60 °C (Figure 3B). These structures likely represent slipped intermolecular or noncanonical states, and not intramolecular structures, due to the very short length and lack of Watson−Crick pairing potential. A T_m of 60 °C is difficult to explain other than by formation of noncanonical or intermolecular multimer structures. At four repeats, the same RNA used for crystallography, two main structures emerged with T_m values at ~50 and 80 °C, with a small fraction of the 60 °C T_m species remaining. As length was increased to 10 repeats, a major structure predominated with a T_m of 78 °C. DSC of our model four-repeat RNA, $[(CCCCGG)_3CCCC]$, annealed to a perfect complement to generate A-form duplex RNA resulted in detection of a single well-defined structure with a T_m of 109 °C (Figure S2B). These results suggest that the structure formed by increasing repeat numbers is an A-form-like structure that likely contains mismatches that reduce stability. Both CD and DSC are consistent with our crystal structures. Together, results suggest that long disease-associated $(CCCCGG)_n$ repeat RNA will favor formation of A-form-like structures with regularly spaced tandem C:C mismatches under physiological conditions.

Repeat RNA sequences have the potential to form non-canonical or non-Watson−Crick structures. However, structural studies of naturally occurring repeat expansion RNAs almost invariably capture A-form-like helical architectures.[6] Solely on the basis of existing trinucleotide repeat RNA structures, single C:C pairs separated by two G-C/C-G base pairs might have been predicted for the C9ORF72 antisense RNA.[6,28] However, thermodynamic considerations predict that the longest runs of the most stable base pairs will be favored with a minimization of the least stable base pairs. In the case of the c9FTD/ALS antisense repeat RNA, this resulted in thermodynamically favored tandem C:C pairing. Watson−Crick hybridization is a cooperative process that likely explains the propensity for repeat expansion RNA to prefer helical structures as repeat number and RNA length increase.[29,30]

Focal aggregation of C9ORF72 antisense repeat RNA in the nucleus and RAN translation in the cytoplasm are linked to interactions with RNA binding proteins. The unique structure and electrostatic surface potential caused by tandem C:C pairs may serve to attract proteins that specifically recognize these features. For example, MBNL-1 protein sequestered by CUG repeat RNA foci naturally recognizes arrays of GC dinucleotides.[31,32] Potentially specific interacting factors have been identified for the sense and antisense c9FTD/ALS repeat RNAs, such as subsets of hnRNP proteins.[33] Alternatively, because C9ORF72 antisense RNA is similar to canonical A-form helices, it may bind a variety of nonspecific proteins. Protein interactions primarily for the G-rich sense RNA have identified proteins with mixed binding specificities.[34,35] Although still unknown, the mechanism of RAN translation may involve extended A-form-like structures that somehow facilitate translation across diverse repeat expansions.[5]

Potential mechanisms of c9FTD/ALS center around C9ORF72 repeat expansion RNA as an initiator for a cascade of molecular disease.[34] Thus, methods for blocking production or toxicity of the repeat expansion RNA hold promise for therapeutic development. Our structure provides opportunities for engineering of such molecules. For example, antisense oligonucleotides and small interfering RNAs that bind targets through Watson−Crick pairing may exhibit enhanced targeting by placing appropriate chemical modifications on the corresponding guanine nucleotides that would bind tandem C:C pairs.[36] Likewise, small molecules may be developed that can uniquely target the C9ORF72 antisense repeat RNA. Molecules previously designed to target CUG or CCUG repeat RNA may serve as a starting point by altering recognition to prefer tandem C:C mismatches and increasing linkers to accommodate four G-C/C-G base pair spacers.[7,10,37] Alternatively, molecules could be identified by screens similar to those designed by Disney and co-workers.[38] Specific binding of molecules to the C9ORF72 antisense repeat RNA is expected to alter RNA structure or protein interactions, which is an important step toward RNA-targeted therapeutics for c9FTD/ALS.

DOI: 10.1021/acs.biochem.6b00136
Biochemistry 2016, 55, 1283−1286

■ ASSOCIATED CONTENT

Supporting Information

The Supporting Information is available free of charge on the ACS Publications website at DOI: 10.1021/acs.biochem.6b00136.

Experimental details and supporting data (PDF)

Accession Codes

Structures have been deposited in the Protein Data Bank as entries 5EW4 and 5EW7.

■ AUTHOR INFORMATION

Corresponding Author

*E-mail: ktgagnon@siu.edu.

Author Contributions

D.W.D. and D.R.T. contributed equally to this work.

Funding

Funding was provided by an ALS Association grant to K.T.G. (16-IIP-260), an ALS Association grant to D.R.C. (2161), and an Isis Pharmaceuticals-sponsored Life Sciences Research Foundation fellowship to D.W.D.

Notes

The authors declare no competing financial interest.

■ ACKNOWLEDGMENTS

Crystal diffraction data were collected at Argonne National Laboratory, Structural Biology Center, at the Advanced Photon Source. Argonne is operated by UChicago Argonne, LLC, for the U.S. Department of Energy, Office of Biological and Environmental Research, under Contract DE-AC02-06CH11357.

■ REFERENCES

(1) van Blitterswijk, M., DeJesus-Hernandez, M., and Rademakers, R. (2012) *Curr. Opin. Neurol. 25*, 689−700.
(2) Zhao, X. N., and Usdin, K. (2015) *DNA Repair 32*, 96−105.
(3) Gendron, T. F., Belzil, V. V., Zhang, Y. J., and Petrucelli, L. (2014) *Acta Neuropathol. 127*, 359−376.
(4) Wojciechowska, M., and Krzyzosiak, W. J. (2011) *Hum. Mol. Genet. 20*, 3811−3821.
(5) Cleary, J. D., and Ranum, L. P. (2014) *Curr. Opin. Genet. Dev. 26*, 6−15.
(6) Kiliszek, A., and Rypniewski, W. (2014) *Nucleic Acids Res. 42*, 8189−8199.
(7) Childs-Disney, J. L., Yildirim, I., Park, H., Lohman, J. R., Guan, L., Tran, T., Sarkar, P., Schatz, G. C., and Disney, M. D. (2014) *ACS Chem. Biol. 9*, 538−550.
(8) Rypniewski, W., Banaszak, K., Kulinski, T., and Kiliszek, A. (2016) *RNA 22*, 22−31.
(9) Park, H., Gonzalez, A. L., Yildirim, I., Tran, T., Lohman, J. R., Fang, P., Guo, M., and Disney, M. D. (2015) *Biochemistry 54*, 3851−3859.
(10) Childs-Disney, J. L., Hoskins, J., Rzuczek, S. G., Thornton, C. A., and Disney, M. D. (2012) *ACS Chem. Biol. 7*, 856−862.
(11) Gendron, T. F., Bieniek, K. F., Zhang, Y. J., Jansen-West, K., Ash, P. E., Caulfield, T., Daughrity, L., Dunmore, J. H., Castanedes-Casey, M., Chew, J., Cosio, D. M., van Blitterswijk, M., Lee, W. C., Rademakers, R., Boylan, K. B., Dickson, D. W., and Petrucelli, L. (2013) *Acta Neuropathol. 126*, 829−844.
(12) DeJesus-Hernandez, M., Mackenzie, I. R., Boeve, B. F., Boxer, A. L., Baker, M., Rutherford, N. J., Nicholson, A. M., Finch, N. A., Flynn, H., Adamson, J., Kouri, N., Wojtas, A., Sengdy, P., Hsiung, G. Y. R., Karydas, A., Seeley, W. W., Josephs, K. A., Coppola, G., Geschwind, D. H., Wszolek, Z. K., Feldman, H., Knopman, D. S., Petersen, R. C., Miller, B. L., Dickson, D. W., Boylan, K. B., Graff-Radford, N. R., and Rademakers, R. (2011) *Neuron 72*, 245−256.
(13) Zu, T., Liu, Y., Banez-Coronel, M., Reid, T., Pletnikova, O., Lewis, J., Miller, T. M., Harms, M. B., Falchook, A. E., Subramony, S. H., Ostrow, L. W., Rothstein, J. D., Troncoso, J. C., and Ranum, L. P. (2013) *Proc. Natl. Acad. Sci. U. S. A. 110*, E4968−4977.
(14) Mori, K., Arzberger, T., Grasser, F. A., Gijselinck, I., May, S., Rentzsch, K., Weng, S. M., Schludi, M. H., van der Zee, J., Cruts, M., Van Broeckhoven, C., Kremmer, E., Kretzschmar, H. A., Haass, C., and Edbauer, D. (2013) *Acta Neuropathol. 126*, 881−893.
(15) Mori, K., Weng, S. M., Arzberger, T., May, S., Rentzsch, K., Kremmer, E., Schmid, B., Kretzschmar, H. A., Cruts, M., Van Broeckhoven, C., Haass, C., and Edbauer, D. (2013) *Science 339*, 1335−1338.
(16) Reddy, K., Schmidt, M. H., Geist, J. M., Thakkar, N. P., Panigrahi, G. B., Wang, Y. H., and Pearson, C. E. (2014) *Nucleic Acids Res. 42*, 10473−10487.
(17) Fratta, P., Mizielinska, S., Nicoll, A. J., Zloh, M., Fisher, E. M. C., Parkinson, G., and Isaacs, A. M. (2012) *Sci. Rep. 2*, 1016.
(18) Reddy, K., Zamiri, B., Stanley, S. Y. R., Macgregor, R. B., and Pearson, C. E. (2013) *J. Biol. Chem. 288*, 9860−9866.
(19) Snoussi, K., Nonin-Lecomte, S., and Leroy, J. L. (2001) *J. Mol. Biol. 309*, 139−153.
(20) Xia, T., McDowell, J. A., and Turner, D. H. (1997) *Biochemistry 36*, 12486−12497.
(21) Kiliszek, A., Kierzek, R., Krzyzosiak, W. J., and Rypniewski, W. (2012) *Nucleic Acids Res. 40*, 8155−8162.
(22) Zheng, G., Lu, X. J., and Olson, W. K. (2009) *Nucleic Acids Res. 37*, W240−246.
(23) Tavares, T. J., Beribisky, A. V., and Johnson, P. E. (2009) *RNA 15*, 911−922.
(24) Vorlickova, M., Kejnovska, I., Sagi, J., Renciuk, D., Bednarova, K., Motlova, J., and Kypr, J. (2012) *Methods 57*, 64−75.
(25) Spink, C. H. (2015) *Methods 76*, 78−86.
(26) Ploeser, J. M., and Loring, H. S. (1949) *J. Biol. Chem. 178*, 431−437.
(27) Mooers, B. H., Logue, J. S., and Berglund, J. A. (2005) *Proc. Natl. Acad. Sci. U. S. A. 102*, 16626−16631.
(28) Su, Z., Zhang, Y., Gendron, T. F., Bauer, P. O., Chew, J., Yang, W. Y., Fostvedt, E., Jansen-West, K., Belzil, V. V., Desaro, P., Johnston, A., Overstreet, K., Oh, S. Y., Todd, P. K., Berry, J. D., Cudkowicz, M. E., Boeve, B. F., Dickson, D., Floeter, M. K., Traynor, B. J., Morelli, C., Ratti, A., Silani, V., Rademakers, R., Brown, R. H., Rothstein, J. D., Boylan, K. B., Petrucelli, L., and Disney, M. D. (2014) *Neuron 83*, 1043−1050.
(29) Ouldridge, T. E., Sulc, P., Romano, F., Doye, J. P., and Louis, A. A. (2013) *Nucleic Acids Res. 41*, 8886−8895.
(30) Saenger, W. (1984) *Principles of Nucleic Acid Structure*, Springer-Verlag, New York.
(31) Goers, E. S., Purcell, J., Voelker, R. B., Gates, D. P., and Berglund, J. A. (2010) *Nucleic Acids Res. 38*, 2467−2484.
(32) Teplova, M., and Patel, D. J. (2008) *Nat. Struct. Mol. Biol. 15*, 1343−1351.
(33) Mori, K., Lammich, S., Mackenzie, I. R., Forne, I., Zilow, S., Kretzschmar, H., Edbauer, D., Janssens, J., Kleinberger, G., Cruts, M., Herms, J., Neumann, M., Van Broeckhoven, C., Arzberger, T., and Haass, C. (2013) *Acta Neuropathol. 125*, 413−423.
(34) Haeusler, A. R., Donnelly, C. J., Periz, G., Simko, E. A., Shaw, P. G., Kim, M. S., Maragakis, N. J., Troncoso, J. C., Pandey, A., Sattler, R., Rothstein, J. D., and Wang, J. (2014) *Nature 507*, 195−200.
(35) Lee, Y. B., Chen, H. J., Peres, J. N., Gomez-Deza, J., Attig, J., Stalekar, M., Troakes, C., Nishimura, A. L., Scotter, E. L., Vance, C., Adachi, Y., Sardone, V., Miller, J. W., Smith, B. N., Gallo, J. M., Ule, J., Hirth, F., Rogelj, B., Houart, C., and Shaw, C. E. (2013) *Cell Rep. 5*, 1178−1186.
(36) Hu, J., Liu, J., Li, L., Gagnon, K. T., and Corey, D. R. (2015) *Chem. Biol. 22*, 1505−1511.
(37) Nguyen, L., Luu, L. M., Peng, S., Serrano, J. F., Chan, H. Y., and Zimmerman, S. C. (2015) *J. Am. Chem. Soc. 137*, 14180−14189.
(38) Rzuczek, S. G., Southern, M. R., and Disney, M. D. (2015) *ACS Chem. Biol. 10*, 2706−2715.

DOI: 10.1021/acs.biochem.6b00136
Biochemistry 2016, 55, 1283−1286